Spin tunneling through an indirect barrier: Tight-binding calculations

Titus Sandu,[1,*] Athanasios Chantis,[2] and Radu Iftimie[1]

[1]*Département de Chimie, Université de Montréal, Case Postale 6128, succursale Centre-ville, Montréal, Québec,
Canada H3C 3J7, Canada*
[2]*Department of Chemical and Materials Engineering, Arizona State University, Tempe, Arizona 85287, USA*

Spin-dependent tunneling through an indirect-band-gap barrier like the GaAs/AlAs/GaAs heterostructure along the [001] direction is studied by the tight-binding method. The tunneling is characterized by the proportionality of the Dresselhaus Hamiltonians at the Γ and X points in the barrier and by Fano resonances (i.e., pairs of resonances and antiresonances or zeros in transmission). The present results suggest that large spin polarization can be obtained for energy windows that significantly exceed the spin splitting. The widths of these energy windows are mainly determined by the energy difference between the resonance and its associated zero, which in turn increases with the decrease of barrier transmissibility at direct tunneling. We formulate two conditions that are necessary for the existence of energy windows with large polarization. First, the resonances must be well separated such that their corresponding zeros are not pushed away from the real axis by mutual interaction. Second, the relative energy order of the resonances in the two spin channels must be the same as the order of their corresponding zeros. The degree to which the first condition is satisfied is determined by the barrier width and the longitudinal effective mass at the X point. In contrast, the second condition can be satisfied by choosing an appropriate combination of spin splitting strength at the X point and transmissibility through the direct barrier.

PACS number(s): 72.25−b, 72.10.Bg, 73.21.Fg, 73.21.Ac

I. INTRODUCTION

The spin rather than the charge of carriers has attracted a lot of interest leading to a new field of electronics dubbed spintronics.[1,2] In this context, spin-polarized transport in nonmagnetic semiconductor structures and spin-dependent properties originating from the spin-orbit interaction are a promising road to spin-based devices.[3]

Despite the progress that has been made,[4,5] spin injection from ferromagnetic leads proved to be very challenging.[6] Consequently, spin-dependent transport in nanostructures comprised of nonmagnetic semiconductors has been the focus of extensive work in recent years.[3] Recent theoretical research has suggested that the current resulting from electron tunneling through zinc-blende semiconductor single-[7,8] or double-barrier structures[9] can be highly spin polarized. The origin of the spin-dependent tunneling in these structures stems from the fact that the barrier material lacks a center of inversion.

In the effective-mass approximation, the electron Hamiltonian of a zinc-blende structure has an additional spin-dependent k^3 coupling called the Dresselhaus term,[10]

$$H_D = \gamma[\sigma_x k_x(k_y^2 - k_z^2) + \sigma_y k_y(k_z^2 - k_x^2) + \sigma_z k_z(k_x^2 - k_y^2)], \quad (1)$$

where σ_i are the Pauli matrices, and k_x, k_y, and k_z are the components of the electron wave vector. For a barrier along the [001] direction the Dresselhaus Hamiltonian is reduced to

$$H_D = \gamma(\sigma_x k_x - \sigma_y k_y)\frac{\partial^2}{\partial^2 z^2}. \quad (2)$$

Perel, Tarasenko, and co-workers[7,8] showed that the Γ point Hamiltonian in Eq. (2) induces an effective-mass correction

leading to a spin-polarized transmission. It is important to emphasize that the spin-dependent part of the effective-mass Hamiltonian at the X point is[10,11]

$$H_D^X = \beta(\sigma_x k_x - \sigma_y k_y) \quad (3)$$

and therefore proportional to the Hamiltonian in Eq. (2). The Hamiltonians in Eqs. (2) and (3) are diagonalized by

$$\chi_{\pm} = \frac{1}{\sqrt{2}}\begin{pmatrix} 1 \\ \mp e^{-i\varphi} \end{pmatrix} \quad (4)$$

with φ the polar angle of the wave vector k_t in the xy plane. Therefore the spin states are not mixed by the interaction between X states and Γ states in the barrier.

Spin-dependent transport can be studied using numerous treatments such as the $k \cdot p$ approach, full-band tight-binding calculations, and *ab initio* methods. For various reasons the theoretical study of spin tunneling through an indirect barrier like GaAs/AlAs/GaAs has not been fully addressed before. $k \cdot p$ cannot fully address the problem because the AlAs barrier accommodates at least one quasibound state into the X valley. Thus, in addition to the Γ-Γ-Γ tunneling, which occurs through the higher Γ valley, one must also consider the tunneling (Γ-X-Γ) through the lower X barrier (see Fig. 1). The $k \cdot p$ method is a perturbative method that can be "tuned" for the necessities of spin-dependent processes (for instance, see Ref. 12, in which spin-dependent evanescent states in the band gap are studied). In contrast, empirical tight-binding methods provide a treatment of the full Brillouin zone, but they lack the complete description of the Dresselhaus term when the spin-orbit coupling is introduced.[13] This is due to
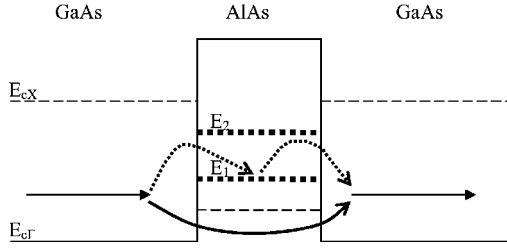
GaAs   AlAs   GaAs

E_{cX}

E_2

E_1

$E_{c\Gamma}$

FIG. 1. Tunneling through the GaAs/AlAs/GaAs barrier. Γ band edges are shown by solid lines and X band edges are represented by dashed lines. E_1 and E_2 are X-valley quasibound states in the AlAs barrier. Direct tunneling (Γ-Γ-Γ) is shown by the solid curly arrow and Γ-X-Γ tunneling is depicted by the dotted curly arrows.

the fact that the orthogonality assumption in tight-binding models is incompatible with the formulation of the spin-orbit interaction.[14] In principle, the above shortcomings should be overcome by utilizing *ab initio* density functional theory methods. However, these methods suffer on the side of band-gap reproducibility.[15]

Spin-dependent tunneling has been recently analyzed with a one-band envelope-function model.[16] In their study,[16] the authors neglected the (Γ-Γ-Γ) tunneling and the presence of X-valley quasibound states in the AlAs barrier. However, spin tunneling through the indirect barrier of the GaAs/AlAs/GaAs heterostructure shows another peculiar property. The confined X states in the AlAs barrier interact[17] with the continuum Γ states in GaAs forming Fano resonances[18] (i.e., pairs of resonances and antiresonances). In this paper we demonstrate that one can use the proximity in the resonance and antiresonance states in conjunction with the spin splitting produced by the spin-dependent Hamiltonian to obtain a large degree of spin polarization within the range between the resonance and antiresonance energies. For this purpose we devise a spin-dependent tight-binding model that provides a realistic view of the spin-dependent tunneling through an indirect barrier. We convert the spin-dependent effective-mass Hamiltonians for a single band to their tight-binding versions following the recipes of Ref. 19. The coupling between Γ and X valleys is made according to Ref. 20.

The paper is organized as follows. In the next section a simple model is analyzed in order to gain insight into the

physics of spin-dependent tunneling. The third section contains a realistic tight-binding model and the numerical results. Conclusions are drawn in the fourth section.

II. TIGHT-BINDING MODEL OF SPIN-DEPENDENT TUNNELING

Consider a simple tight-binding (TB) model of the spin-dependent tunneling through an indirect barrier. The main assumptions for this TB model are that spin states are degenerate in left and right leads (bulklike states) and the Dresselhaus Hamiltonians are proportional for Γ and X states in the barrier, so we can assume that the spin states in the leads are eigenvectors of the Dresselhaus Hamiltonian.

A. Spin tunneling through an indirect barrier

The Hamiltonian of the system is

$$H = \sum_{n=-\infty,\sigma=\uparrow,\downarrow}^{-1} \left[\varepsilon c_{n,\sigma}^\dagger c_{n,\sigma} + (t c_{n-1,\sigma}^\dagger c_{n,\sigma} + \text{H. c.}) \right]$$
$$+ \sum_{n=1,\sigma=\uparrow,\downarrow}^{\infty} \left[\varepsilon c_{n,\sigma}^\dagger c_{n,\sigma} + (t c_{n,\sigma}^\dagger c_{n+1,\sigma} + \text{H. c.}) \right] + \varepsilon_1 c_{0,\uparrow}^\dagger c_{0,\uparrow}$$
$$+ \varepsilon_2 c_{0,\downarrow}^\dagger c_{0,\downarrow} + (V_1 c_{0,\uparrow}^\dagger c_{-1,\uparrow} + V_2 c_{0,\downarrow}^\dagger c_{-1,\downarrow} + \text{H. c.})$$
$$+ (V_1 c_{0,\uparrow}^\dagger c_{1,\uparrow} + V_2 c_{0,\downarrow}^\dagger c_{1,\downarrow} + \text{H. c.}) + (t_1 c_{-1,\uparrow}^\dagger c_{1,\uparrow}$$
$$+ t_2 c_{-1,\downarrow}^\dagger c_{1,\downarrow} + \text{H. c.}). \tag{5}$$

The first two terms on the right-hand side of Eq. (5) are the Hamiltonians of the contacts (leads), where ε and t are the on-site energy and transfer integral, respectively (spin degenerate). $c_{n\sigma}^\dagger$ ($c_{n\sigma}$) is the creation (annihilation) operator of an electron with spin σ on site n. The remaining part is the Hamiltonian of the barrier and its coupling to the leads. The active region is modeled by three sites: site -1 that is like the left-hand side contact, site 0 that is the actual barrier, and site 1 that is like the right-hand side contact. Thus the effective left- (right-)hand side contact ends (starts) at site -2 (2). The matrix form of the Hamiltonian for the sites -1, 0, and 1 (in fact $E-H$, where E is the energy) with appropriate boundary conditions for an open system is[21]

	$-1\uparrow$	$-1\downarrow$	$0\uparrow$	$0\downarrow$	$1\uparrow$	$1\downarrow$
$-1\uparrow$	$E-\varepsilon-\Sigma_L(E)$	0	$-V_1$	0	$-t_1$	0
$-1\downarrow$	0	$E-\varepsilon-\Sigma_L(E)$	0	$-V_2$	0	$-t_2$
$E-H=\quad 0\uparrow$	$-V_1^*$	0	$E-\varepsilon_1$	0	$-V_1^*$	0
$0\downarrow$	0	$-V_2^*$	0	$E-\varepsilon_2$	0	$-V_2^*$
$1\uparrow$	$-t_1^*$	0	$-V_1$	0	$E-\varepsilon-\Sigma_R(E)$	0
$1\downarrow$	0	$-t_2^*$	0	$-V_2$	0	$E-\varepsilon-\Sigma_R(E)$

$$(6)$$

where $\Sigma_{L,R}(E)$ are the self-energies of the semi-infinite parts, i.e.,

$$\Sigma_{L,R}(E) = t^\dagger \frac{1}{E - H_{L,R} + i\delta} t, \qquad (7)$$

where $H_{L,R}$ are the Hamiltonians of the semi-infinite left- and right-hand sides and δ is an infinitesimal positive number. The retarded Green function

$$G_{L,R}^R(E) = \frac{1}{E - H_{L,R} + i\delta} \qquad (8)$$

of the left- (right-)hand side semi-infinite contact in Eq. (7) is actually the diagonal part $G_L^R(E)_{-2,-2}$ $[G_R^R(E)_{2,2}]$ representing

the site -2 (2). The expressions of these Green function elements can be found from their equation of motion and the use of the finite-difference equation method.[22] If we consider the parametrization $\varepsilon - E = 2t \cos(ka)$, with k a complex parameter and a a lattice constant parameter, we obtain the following equation for the self-energies:

$$\Sigma_{L,R} = -t e^{ika}. \qquad (9)$$

Therefore, the Green function G^R for the sites -1, 0, and 1 with the boundary conditions for an open system is

$$G^R(E) = \begin{bmatrix} -te^{-ika} & 0 & -V_1 & 0 & -t_1 & 0 \\ 0 & -te^{-ika} & 0 & -V_2 & 0 & -t_2 \\ -V_1^* & 0 & E-\varepsilon_1 & 0 & -V_1^* & 0 \\ 0 & -V_2^* & 0 & E-\varepsilon_2 & 0 & -V_2^* \\ -t_1^* & 0 & -V_1 & 0 & -te^{-ika} & 0 \\ 0 & -t_2^* & 0 & -V_2 & 0 & -te^{-ika} \end{bmatrix}^{-1}. \qquad (10)$$

We notice that the Hamiltonian is not Hermitian due to open boundary conditions. To calculate the transmission probability from site 1 to N we use the formula[21]

$$T(E, k_t) = \Gamma_L(E, k_t) |G_{1,N}^R(E, k_t)|^2 \Gamma_R(E, k_t), \qquad (11)$$

with

$$\Gamma_{L,R}(E, k_t) = i[\Sigma_{L,R}(E, k_t) - \Sigma_{L,R}^*(E, k_t)]. \qquad (12)$$

Since the Dresselhaus Hamiltonians are proportional at the Γ and X points in the barrier[10,11] we can solve separately for each spin. The Green function for spin up is

$$G_\uparrow^R(E) = \begin{bmatrix} -te^{-ika} & -V_1 & -t_1 \\ -V_1^* & E-\varepsilon_1 & -V_1^* \\ -t_1^* & -V_1 & -te^{-ika} \end{bmatrix}^{-1}. \qquad (13)$$

A similar equation is obtained for the spin down. The poles of G^R are the solutions of the determinant equation

$$\Delta = \begin{vmatrix} -te^{-ika} & -V_1 & -t_1 \\ -V_1^* & E-\varepsilon_1 & -V_1^* \\ -t_1^* & -V_1 & -te^{-ika} \end{vmatrix} = 0, \qquad (14)$$

while the zeros of the transmission are the zeros of the Green function $(G_\uparrow^R)_{1,3}$ relating the sites -1 and 1,

$$(G_\uparrow^R)_{1,3}(E) = \frac{\begin{vmatrix} -V_1 & E-\varepsilon_1 \\ -t_1 & -V_1^* \end{vmatrix}}{\Delta} = 0. \qquad (15)$$

The equation for the poles reads

$$(E - \varepsilon_1)(|t_1|^2 - t^2 e^{-2ika}) = |V_1|^2(-t_1 - t_1^* + 2te^{-ika}) \qquad (16)$$

and for the zeros

$$(E - \varepsilon_1)t_1 = -|V_1|^2. \qquad (17)$$

Since t is basically the conduction bandwidth and t_1 and V_1 are tunneling rates, then $V_1, t_1 \ll t$, such that the pole is given by

$$E \approx \varepsilon_1 - 2\frac{|V_1|^2}{t} e^{ika}. \qquad (18)$$

The equation for the zero is

$$E = \varepsilon_1 - \frac{|V_1|^2}{t_1}. \qquad (19)$$

Since we have $V_1, t_1 \ll t$, the energy separation between the pole and the zero is about V_1^2/t_1. The resonances and zeros occur at slightly different energies for the two spin channels, resulting in a large spin polarization due to the combination of a sharp increase in transmission at resonance followed by an abrupt decrease to zero at antiresonance. Hence, the energy range of large spin polarization will depend on V_1 and t_1 but not on the magnitude of spin splitting. One can notice that the energy separation between resonance and antiresonance can be increased by decreasing t_1, i.e., increasing the width of the barrier. In Fig. 2 we illustrate the above arguments with the parameters given in Table I. We also calculate the spin polarization with the equation
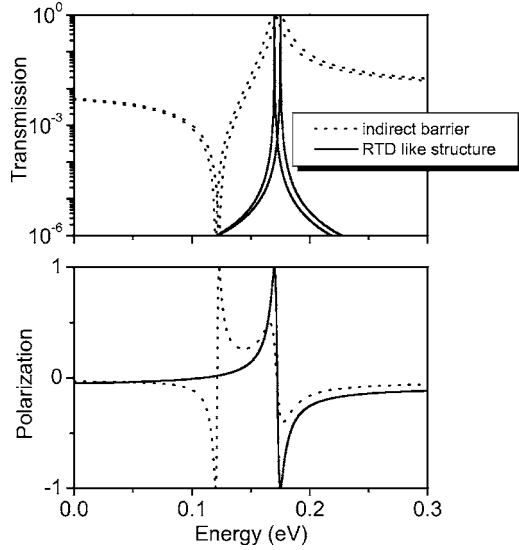
FIG. 2. Spin-dependent transmission (upper panel) and spin polarization (lower panel) through an indirect barrier versus a resonant tunneling diode configuration. One can see the wide energy window of large polarization created by indirect tunneling.

$$P = \frac{T_\uparrow - T_\downarrow}{T_\uparrow + T_\downarrow}. \tag{20}$$

For comparison we also plot the case of the resonance tunneling diode (RTD) configuration. The RTD configuration is made by setting t_1 and t_2 to 0. To separate the spin resonances, we also have chosen the values of V_1 and V_2 ten times smaller than their values in the indirect-barrier configuration. Figure 2 shows that the indirect barrier configuration has a clear advantage over the RTD configuration.

B. Spin tunneling through a direct barrier

Following the same procedure one can also calculate spin transmission through a direct barrier. The Green function of the open system is

TABLE I. Matrix elements in eV of the nearest-neighbor model outlined in Eq. (5).

	Indirect barrier	RTD-like structure
t	1.0	1.0
V_1	0.05	0.005
V_2	0.052	0.0052
t_1	0.05	0.0
t_2	0.052	0.0
ε_1	0.17	0.17
ε_2	0.175	0.175

$$G^R(E) = \begin{bmatrix} -te^{-ika} & 0 & -t_1 & 0 \\ 0 & -te^{-ika} & 0 & -t_2 \\ -t_1^* & 0 & -te^{-ika} & 0 \\ 0 & -t_1^* & 0 & -te^{-ika} \end{bmatrix}^{-1}. \tag{21}$$

The Green function for the spin up is

$$G_\uparrow^R(E) = \begin{bmatrix} -te^{-ika} & -t_1 \\ -t_1^* & -te^{-ika} \end{bmatrix}^{-1}. \tag{22}$$

Using Eqs. (11) and (12) we calculate the spin-dependent transmission probabilities for a direct barrier. The transmission probabilities are approximated by

$$T_\uparrow \approx \frac{4|t_1|^2}{t^2} \sin^2 ka \tag{23}$$

and

$$T_\downarrow \approx \frac{4|t_2|^2}{t^2} \sin^2 ka, \tag{24}$$

i.e., the transmission for spin up is different from transmission for spin down, leading to spin polarization.

III. RESULTS OF A REALISTIC TIGHT-BINDING MODEL AND DISCUSSIONS

In order to make quantitative assessments of the spin tunneling through an indirect barrier, we devise a spin-dependent tight-binding model for a system that is partitioned into layers. The layers from $-\infty$ to 0 and from $N+1$ to ∞ are the contacts, while the layers from 1 to N are the active layers. First, we consider the spin-independent Hamiltonian. The coupling between Γ and X states is treated similarly to Ref. 20, with the Hamiltonian

$$H = \begin{bmatrix} H_\Gamma & H_{\Gamma X} \\ H_{X\Gamma} & H_X \end{bmatrix}. \tag{25}$$

H_Γ and H_X are the Hamiltonians at the Γ and X points, respectively. $H_{\Gamma X}$ and $H_{X\Gamma}$ are the couplings between Γ and X at the interface layers. For simplicity, we do not distinguish between X_1 and X_3, such that H_Γ and H_X are single-band effective-mass Hamiltonians that are converted to TB Hamiltonians according to the parametrization given in Ref. 19. This TB parametrization has been successfully used in quantum transport for nonequilibrium conditions and incoherent scattering processes.[23] The parametrization[19,23] is made for the effective-mass Hamiltonian

$$H_0 = \frac{-\hbar^2}{2} \frac{d}{dz} \frac{1}{m^*(z)} \frac{d}{dz} + V_k(z) + \frac{\hbar^2 k_t^2}{2m_L^*}, \tag{26}$$

where m_L^* is the effective mass in the left contact, the effective mass is considered z dependent, and the spatial dependence of the transverse energy has been incorporated in the transverse-momentum- (k_t-)dependent potential:

$$V_k(z) = V(z) + \frac{\hbar^2 k_t^2}{2m_L^*}\left(\frac{m_L^*}{m(z)} - 1\right). \tag{27}$$

TABLE II. Dresselhaus coefficients at Γ and X points for GaAs and AlAs, calculated with the GW method (Refs. 25 and 26) with spin-orbit coupling included. The units are atomic units.

	GaAs	AlAs
γ(hartree bohr)^3	2.1	0.85
β (hartree bohr)	0.0074	0.00077

The corresponding tight-binding parameters for the non-diagonal part are

$$t_{ij} = \frac{\hbar^2}{(m_i + m_j)\Delta^2} \qquad (28)$$

and the diagonal part is

$$D_i(k_t) = \frac{\hbar^2}{2\Delta^2}\left(\frac{1}{m^+} + \frac{1}{m^-}\right) + V_i(k_t). \qquad (29)$$

In Eqs. (28) and (29), m_i is the effective mass at site i on the mesh of spacing Δ, $V_i(k_t)$ is the potential at site i, which also includes the band offsets, $m^- = (m_{i-1}+m_i)/2$ and $m^+ = (m_i +m_{i+1})/2$. The spin-dependent Hamiltonian is expressed in the basis spanned by spinors (4), such that the Hamiltonian is diagonal in this basis. At the Γ point the spin-dependent part of the effective-mass Hamiltonians is introduced through the corrections to the effective masses defined in Eq. (2) and the effective potential defined in Eq. (27). The spin-dependent part at X is expressed through different band offsets for the two spin projections as one can see from Eq. (3).

Our calculations are performed with the effective masses and band edges taken from Ref. 24. The Dresselhaus parameters given in Table II are calculated with a quasiparticle self-consistent GW (G=Green function, W=screened Coulomb interaction) method as in Refs. 25 and 26 with spin-orbit coupling included perturbatively. The splitting at Γ in GaAs found in the present work with the GW method is three times smaller than the value used by Perel et $al.$ in Ref. 7.[27] The GW spin splitting at Γ for AlAs is about 2.5 times smaller than in GaAs. While for GaAs one can also use the experimental estimation for the splitting at the Γ point[27] there are no such estimations for AlAs. Therefore to be consistent, we used the GW values for both. The value of spin splitting at the X point is almost the same as the one obtained within the local density approximation with our full potential linear muffin-tin orbitals code.[28] The X-Γ band offset for a GaAs/AlAs heterostructure is chosen to be 160 meV.[29] Throughout the paper we have chosen a value $k_t = 2\pi/a \times 0.05$ for the transverse wave vector (a is the lattice constant of GaAs).

In Fig. 3 we compare the one-band model (direct tunneling) given by the effective-mass Hamiltonian and the two-band model (direct and indirect tunneling) given by Eq. (25). Below the indirect barrier, the main contribution to spin tunneling and polarization is provided by direct tunneling. However, the tunneling and the polarization through the X states become dominant for energies above the indirect barrier. The result shows that the confinement of the X states in the bar-
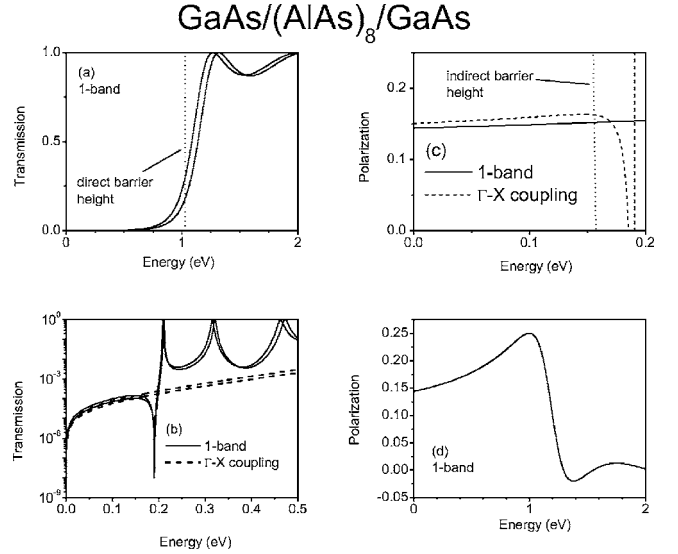

FIG. 3. (a) Spin-dependent transmission probability of one-band (direct) tunneling through GaAs/(AlAs)$_8$/GaAs barrier. (b) Comparison between full (direct and indirect) and one-band (direct) transmission probabilities of a GaAs/(AlAs)$_8$/GaAs barrier. (c) Comparison of spin polarization between full (direct and indirect) and one-band (direct) electron transmission of a GaAs/(AlAs)$_8$/GaAs barrier. (d) Spin polarization obtained from one-band calculation over a broader energy range.

rier increases the energy threshold at which the tunneling through X states becomes dominant. In the calculations[16] in which the confinement of the X states in the barrier is neglected, the tunneling is predominantly indirect for energies slightly below the top of indirect barrier. Therefore, our calculations suggest that multiband calculations are needed to fully describe the electron transport in these heterostructures.

In Fig. 4 we show the transmission probability and spin polarization for GaAs/(AlAs)$_N$/GaAs heterostructures with N=4, 6, and 8. Energy windows with large polarization can be seen between the resonance and its corresponding zero.
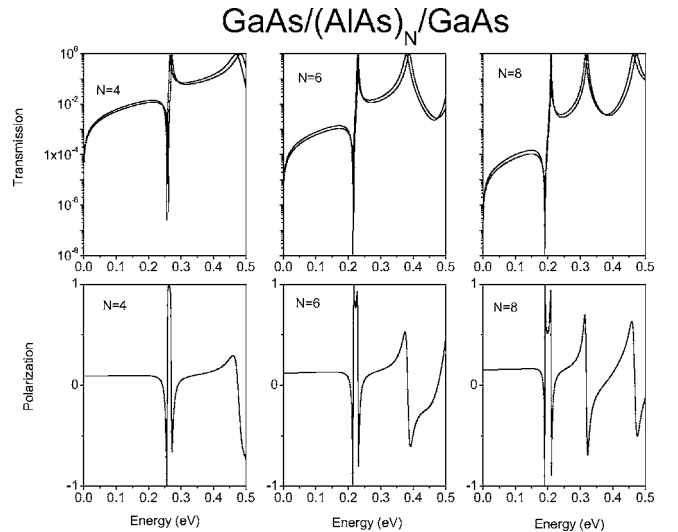

FIG. 4. Spin-dependent transmission probability and spin polarization of a GaAs/(AlAs)$_N$/GaAs heterostructure. N=4, 6, and 8.
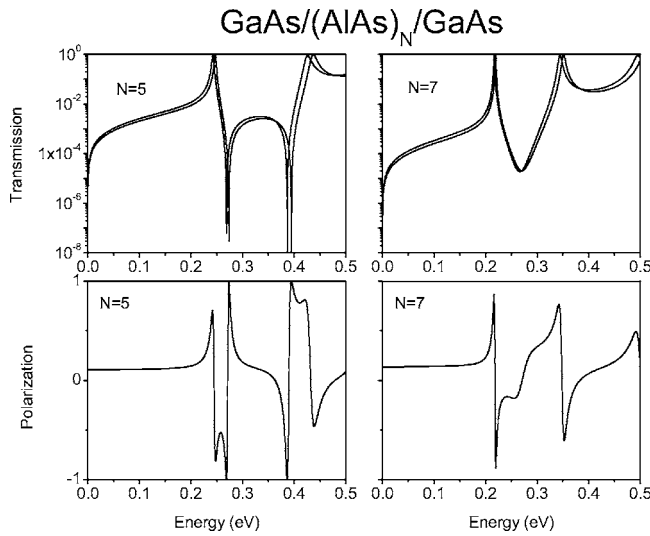
FIG. 5. Spin-dependent transmission probability and spin polarization of a GaAs/$(AlAs)_N$/GaAs heterostructure. $N=5$ and 7.

FIG. 6. Comparison of spin-dependent transmission probability and spin polarization between GaAs/$(AlAs)_{12}$/GaAs and GaAs/$(Al_{0.8}Ga_{0.2}As)_{12}$/GaAs heterostructures.

The width of the window increases with the barrier width as was demonstrated in the previous section. Only the first resonance has a corresponding zero on the real axis; for the other resonances, the zeros are pushed off the real axis.[30] Therefore, if the resonances are close enough, no well-defined window with large spin polarization can be found. The possibility to obtain well-separated resonances with zeros on the real axis is controlled by the combination of the longitudinal effective mass in the barrier at the X point and the barrier width. A lighter longitudinal effective mass and/or a narrower barrier push farther apart the resonance energies in the barrier.

In Fig. 5 we plot the transmission probability and spin polarization for GaAs/$(AlAs)_N$/GaAs with $N=5$ and 7. The parity of the number of AlAs monolayers has been taken into account.[20] The case $N=5$ shows two wide windows with large and opposite spin polarizations. Again, the polarization windows are mainly determined by the resonance and antiresonance positions and not by the magnitude of spin splitting. However, $N=7$ shows no such energy windows because the zeros have moved away from the real axis. Moreover, at larger values of N no energy windows with large polarization are found for both even and odd values of N.

The pattern can be reestablished by increasing the strength of the Dresselhaus coefficient at the X point in the barrier. A barrier made of $Al_{0.8}Ga_{0.2}As$ can achieve this goal. In $Al_{0.8}Ga_{0.2}As$, the Dresselhaus coefficients are mixtures of those of AlAs and GaAs. GaAs has larger coefficients, in particular, β is ten times larger than the β coefficient of AlAs, making the β coefficient of the compound stronger than that of AlAs. In Fig. 6 we make a comparison between $Al_{0.8}Ga_{0.2}As$ and AlAs barriers with a thickness of $N=12$ monolayers. The virtual crystal approximation was employed to calculate the physical parameters of $Al_{0.8}Ga_{0.2}As$. This is a reasonable assumption, since AlAs and GaAs have similar structural and electronic properties. Figure 6 illustrates clearly that the $Al_{0.8}Ga_{0.2}As$ barrier shows a window of polarization, while the AlAs barrier does not.

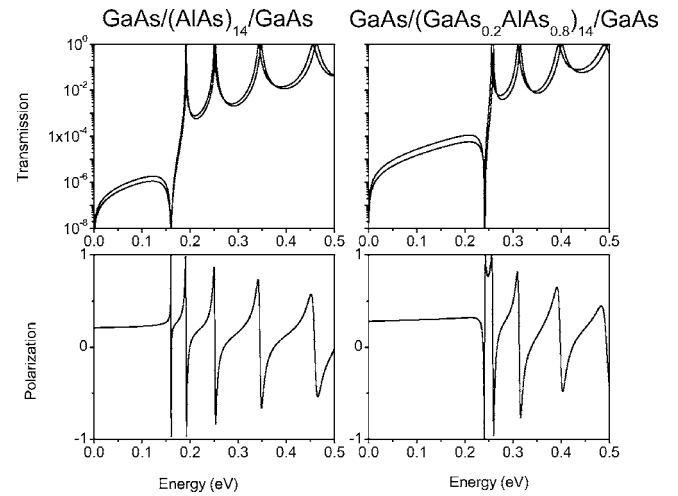Visual analysis of Figs. 6 and 7 suggests that in order to obtain polarization windows, the resonances and zeros in the spin channels must be properly ordered. If a resonance is occurring first in the spin channel 1, the zero in the transmission coefficient of the spin channel 1 must precede the zero in the transmission coefficient of spin channel 2. This condition is satisfied for wider barriers provided that the Dresselhaus coefficient at the X point is sufficiently large.

The practical aspect of focusing the electrons to energies within the large-polarization window can be achieved by placing a RTD structure in front of the tunneling barrier. In this way, one not only can control the incoming energy of the electrons but also ensures that most electrons have nonvanishing transverse momenta[31] and, consequently, their energies are spin split.

It is important to analyze at this point the influence that the neglect of the Dresselhaus k^3 term in the leads can have
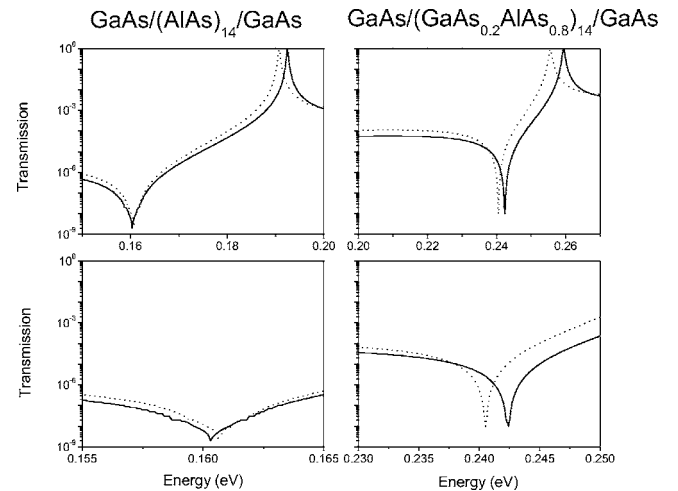

FIG. 7. Closer look at spin-dependent transmission probability around the resonance energy for GaAs/$(AlAs)_{12}$/GaAs and GaAs/$(Al_{0.8}Ga_{0.2}As)_{12}$/GaAs heterostructures. It explains the origin of the energy window with large spin polarization.

on the conclusions drawn in the present work. Since the tight-binding basis is localized, different bases can be used to treat the spin Hamiltonian in the barrier and in the leads. In the leads, the basis is that which makes diagonal the Hamiltonian in Eq. (2), while in the barrier the basis is given in Eq. (4). The nondiagonal spin-dependent part is then transferred to interface terms between leads and barrier. The corrections to the Green function and transmission coefficients are quadratic with respect the strength of this nondiagonal term. This analysis indicates that the conclusions of the paper are not likely to change if the Dresselhaus term in the leads is properly taken into account. A detailed quantitative discussion will be presented elsewhere since special care must be exercised due to the presence of the k_z-linear term in Eq. (2).

IV. CONCLUSIONS

We investigated the spin-dependent transport across an indirect semiconductor barrier of a zinc-blende structure like the GaAs/AlAs/GaAs heterostructure along the [001] axis by means of a combination of several tight-binding models. Spin tunneling through such an indirect barrier exhibits two major characteristics: the proportionality of the Dresselhaus Hamiltonians at the Γ and X points and the Fano resonances. A generic tight-binding Hamiltonian has shown that large spin polarization occurs in the energy window determined by the separation between the resonance and its associated antiresonance and not because of the magnitude of the spin splitting of resonances. Moreover, the energy separation between the resonance and its corresponding antiresonance increases as the barrier width increases.

Realistic calculations have been performed with a two-band tight-binding model. The effective mass Hamiltonians at Γ and X have been converted[19] to tight-binding Hamiltonians. The Γ-X coupling was implemented following the scheme presented in Ref. 20. Accordingly, the Dresselhaus Hamiltonians at Γ and X in the barrier have been included in the effective masses and band offsets. The calculations show that, in order to obtain energy windows with large polarization, two conditions need to be satisfied. The first condition consists of having well-separated resonances such that their corresponding antiresonances do not interact with each other. The second condition is that the relative energy order of the resonances in the two spin channels must be the same as the order of their corresponding zeros. The first condition is achieved by an appropriate combination of barrier width and longitudinal effective mass at the X point, while the second condition is accomplished by a combination of spin splitting strength at the X point and transmissibility through the direct barrier.

Electrons can be focused in the required energy windows by passing them through a resonant tunneling diode structure situated in front of the indirect barrier. Using such an experimental setup, one could obtain large spin polarization following the procedure of Perel *et al.*[7] and Glazov *et al.*[9]

*Electronic address: titus.sandu@umontreal.ca

[1] S. Wolf, D. Awschalom, R. Buhrman, J. Daughton, S. von Molnar, M. Roukes, A. Chtchelkanova, and D. Treger, Science **294**, 1488 (2001).

[2] I. Zutic, J. Fabian, and S. D. Sarma, Rev. Mod. Phys. **76**, 323 (2004).

[3] *Semiconductor Spintronics and Quantum Computation*, edited by D. Awschalom, D. Loss, and N. Samarth (Springer, Berlin, 2002).

[4] E. I. Rashba, Phys. Rev. B **62**, R16267 (2000).

[5] A. Hanbicki, B. Jonker, G. Itskos, G. Kioseoglou, and A. Petrou, Appl. Phys. Lett. **80**, 1240 (2002).

[6] G. Schmidt, D. Ferrand, L. W. Molenkamp, A. T. Filip, and B. J. van Wees, Phys. Rev. B **62**, R4790 (2000).

[7] V. I. Perel, S. A. Tarasenko, I. N. Yassievich, S. D. Ganichev, V. V. Belkov, and W. Prettl, Phys. Rev. B **67**, 201304(R) (2003).

[8] S. A. Tarasenko, V. I. Perel, and I. N. Yassievich, Phys. Rev. Lett. **93**, 056601 (2004).

[9] M. M. Glazov, P. S. Alekseev, M. A. Odnoblyudov, V. M. Chistyakov, S. A. Tarasenko, and I. N. Yassievich, Phys. Rev. B **71**, 155313 (2005).

[10] G. Dresselhaus, Phys. Rev. **100**, 580 (1955).

[11] E. L. Ivchenko and G. E. Pikus, *Superlattices and Other Heterostructures: Symmetry and Optical Phenomena*, 2nd ed. (Springer, Berlin, 1997).

[12] N. Rougemaille, H. -J. Drouhin, S. Richard, G. Fishman, and A. K. Schmid, Phys. Rev. Lett. **95**, 186406 (2005).

[13] T. B. Boykin, Phys. Rev. B **57**, 1620 (1998).

[14] T. Sandu, Phys. Rev. B **72**, 125105 (2005).

[15] R. Jones and O. Gunnarsson, Rev. Mod. Phys. **61**, 689 (1989).

[16] S. Mishra, S. Thulasi, and S. Satpathy, Phys. Rev. B **72**, 195347 (2005).

[17] R. Beresford, L. F. Luo, W. I. Wang, and E. E. Mendez, Appl. Phys. Lett. **55**, 1555 (1989).

[18] U. Fano, Phys. Rev. **124**, 1866 (1961).

[19] W. R. Frensley, in *Heterostructures and Quantum Devices*, edited by W. Frensley and N. Einspruch (Academic Press, San Diego, CA, 1994), p. 273.

[20] Y. Fu, M. Willander, E. L. Ivchenko, and A. A. Kiselev, Phys. Rev. B **47**, 13498 (1993).

[21] S. Datta, *Electronic Transport in Mesoscopic Systems* (Cambridge University Press, New York, 1995).

[22] A. B. Chen, Y. M. Lai-Hsu, and W. Chen, Phys. Rev. B **39**, 923 (1989).

[23] R. Lake, G. Klimeck, R. C. Bowen, and D. Jovanovic, J. Appl. Phys. **81**, 7845 (1997).

[24] G. Klimeck, R. C. Bowen, T. B. Boykin, and T. A. Cwik, Superlattices Microstruct. **27**, 519 (2000).

[25] S. V. Faleev, M. van Schilfgaarde, and T. Kotani, Phys. Rev. Lett. **93**, 126406 (2004).

[26] A. N. Chantis, M. van Schilfgaarde, and T. Kotani, cond-mat/0508274 [Phys. Rev. Lett. (to be published)].

[27] G. E. Pikus, V. A. Marushchak, and A. N. Titkov, Sov. Phys. Semicond. **22**, 115 (1988).

[28] M. Methfessel, M. van Schilfgaarde, and R. Casali, in *Electronic Structure and Physical Properties of Solids: The Uses of the LMTO Method*, Lecture Notes in Physics, edited by H. Dreysse (Springer-Verlag, Berlin, 2000), p. 114.

[29] E. E. Mendez, E. Calleja, and W. I. Wang, Appl. Phys. Lett. **53**, 977 (1988).

[30] R. C. Bowen, W. R. Frensley, G. Klimeck, and R. K. Lake, Phys. Rev. B **52**, 2754 (1995).

[31] T. Sandu, G. Klimeck, and W. P. Kirk, Phys. Rev. B **68**, 115320 (2003).